High-temperature photomodulated thermoreflectance measurements on phosphorus implanted and annealed silicon wafers

Andreas Othonos, Constantinos Christofides,[a] and Efi Loizidou
Photonics and Optoelectronics Research Laboratory, Department of Physics, University of Cyprus, P.O. Box 20537, 1678 Nicosia, Cyprus

(Received 20 May 2003; accepted 3 September 2003)

Photomodulated thermoreflectance measurements between 300 and 650 K on phosphorus implanted and annealed silicon wafers are reported. The change of the photothermal amplitude and phase as a function of temperature is discussed. Several measurements have been performed on silicon wafers annealed at various temperatures in the range of 300 to 1100 °C. The activation energy of the local annealing process was also estimated to be 0.17 eV. © *2003 American Institute of Physics.*
[DOI: 10.1063/1.1621723]

I. INTRODUCTION

As it is well known that implantation of impurity atoms for doping semiconductor wafers offers many advantages such as rapidity, mass separation for purity requirements, accuracy and a wide range of doses, flexibility of profile depth, and a control over the amount of ions in a specific region.[1] One of the main disadvantages of ion implantation process is damage introduced into semiconductor resulting from the energetic character of the progress. The consequence of ion implantation is the amorphization of the semiconductor surface and the presence of electrical defects. Ion implantation, therefore, must be followed by an annealing process for the semiconductor to recover its crystallinity and for the doping impurities to become electrically active.[2,3] Over the last three decades, the importance of ion implantation as alternative technique for semiconducting doping has led to the development of many characterization techniques.[2,3]

Since the early 1980's, various photothermal techniques have been developed for the characterization of implanted unannealed and annealed semiconducting wafers. The nondestructive character of these techniques makes them particularly attractive for the nondestructive evaluation of ion-implanted materials. In fact, since the establishment of the photomodulated thermoreflectance (PMTR) technique[4–11] a lot of progress has been made. While the technique was used extensively for room-temperature measurements, attempts were also made for PMTR measurements at wide temperature ranges. Vitkin *et al.*[12] examined the PMTR signal in connection to temperatures obtaining measurements with temperatures ranging between 40–300 K. Five years later, Nestoros *et al.*[13] made a theoretical analysis of the experimental measurements mentioned above. Mandelis *et al.*[14] published a primary theoretical study about the spreading of thermoelectronic waves at high temperatures while Christofides *et al.*[15] published photothermal results obtained at high temperatures. This study forms the first base for the analysis of the behavior of PMTR at high temperatures with a perspective to develop a PMTR instrument for measurements at elevated temperatures. The expansion of the photothermal theory at high temperatures is a very important objective in the field of characterization of semiconducting films and devices. In this case, the technique offers the possibility to materialize measurements during the annealing process of implanted materials and the preparation of thin films. Such a technique would be welcome in the microelectronics industry because it would evaluate the materials nondestructively during the annealing process (crystallization process and the electronic activation of the network, in the case of implanted semiconductors). In addition, the changes of the surface of thin films could be characterized in real time. This technique could also be helpful to material scientists for real time characterization during the growth of semiconducting films.

The aim of this article is to present and interpret results concerning the temperature dependence of the PMTR signal between 300 and 650 K in phosphorus implanted silicon wafers. Section II presents a short review of the photothermal theory while Sec. III is the presentation of the experimental setup and many experimental details about the procedures, the performance of the experiments, and the implanted silicon wafers. Section IV presents experimental results while Sec. V presents a discussion. Finally, some concluding remarks are presented.

II. THEORETICAL BACKGROUND

In this work, the characterization of lightly doped silicon samples at elevated temperatures is reported. As it is well known in typical PMTR experiments, a light pulse from a pump laser source causes an excursion in the local temperature of the sample and this manifests itself as a change in the reflected probe beam. In general, the change in reflectivity is directly related to the heating of the lattice by the pump beam; this heating affects the temperature dependence of the optical constant of the material. In the case of semiconductors, however, there is an additional effect, the creation of electron–hole pairs. We can write the total induced photomodulated contribution as a sum of the thermal and plasma contribution:[4–10]

[a] Electronic mail: ccc@ucy.ac.cy

 © 2003 American Institute of Physics

Downloaded 30 May 2010 to 194.42.23.188. Redistribution subject to AIP license or copyright; see http://jap.aip.org/jap/copyright.jsp

$$\frac{\Delta R}{R_0}=\frac{1}{R_0}\left(\frac{\partial R}{\partial T}\right)\Delta T+\frac{1}{R_0}\left(\frac{\partial R}{\partial N}\right)\Delta N, \tag{1}$$

$$\frac{\Delta R}{R_0}=\frac{\Delta R_{\mathrm{th}}}{R_0}+\frac{\Delta R_{\mathrm{pl}}}{R_0}, \tag{2}$$

where R_0 is the reflectivity at temperature T_0 and plasma density N_0. The first term of the right-hand side of the Eq. (1) is the temperature coefficient of reflectivity, and the second term is the plasma coefficient of reflectivity, which can also be negative. ΔR, ΔT, and ΔN are the local variations of the reflectance, temperature, and plasma density, respectively, induced by the absorption of the laser pump beam. ΔR_{th} and ΔR_{pl} of Eq. (2) are the photothermal signal components due to the thermal and plasma effect, respectively. It has been shown that the photothermal signal will be proportional to the variations in the surface temperature. For resulting signal, in the case of a one-dimensional (1D) analysis, the PMTR amplitude attributed to the thermal contribution may be written as:[12]

$$\frac{\Delta R_{\mathrm{th}}(T)}{R_0}\approx\frac{H}{\sqrt{\omega\rho C\kappa(T)}}, \tag{3}$$

where ρ is the density of the solid, C is the specific heat at constant volume, and κ is the thermal conductivity which depends strongly on temperature. The essentially temperature-independent factor H is a function of the real and imaginary parts of the medium refractive index and the total temperature derivatives of real and imaginary parts of the dielectric constant. We note that the signal is inversely proportional to the square root of angular frequency, $\omega=2\pi f$ (where f is the modulation frequency). It is also inversely proportional to the sample thermal conductivity κ, which is a function of lattice temperature.

The effect of the photogenerated plasma becomes important for $\omega\tau\geqslant 1$, which was also studied by several workers.[4–12] Assuming spatially homogeneous electron–hole plasma, and a simple Drude effect model, the plasma reflectance is expressed in the case of a 1D analysis by

$$\frac{\Delta R_{\mathrm{pl}}(T)}{R_0}\approx-\frac{2\lambda^2 e^2}{\pi m^* \nu_c^2}\frac{\Delta N}{n(n^2-1)}, \tag{4}$$

where e^- is the electron charge, m^* is the effective mass of the electron, ν_c is the velocity of the light, and λ is the optical wavelength of the probe laser. The temperature-varying parameters in Eq. (4) are the real part of the refractive index, n, and the excess plasma density, ΔN. Figure 1 presents the variation of the term $[n(n^2-1)]^{-1}$ versus temperature in the range of 300 to 650 K. In fact, this term varies from 0.0198 to 0.0199; this variation is less than 2% between 294 K and 623 K.[16] As a result, it is obvious that any variation of the plasma component versus temperature is going to depend only on the variation of ΔN term.

It is well known that, in the case of low modulation frequency $(\omega\tau\ll 1)$, the PMTR signal is dominated completely by the thermal contribution. On the other hand, at higher frequency, $(\omega\tau\geqslant 1)$, we have a competition between thermal and plasma effects. In this work, we present the extension of the conventional laser-induced photomodulated thermoreflectance method for measurements at elevated temperatures. The PMTR signal is simply the change in modulated reflectance, ΔR and not the normalized reflectance signal, $\Delta R_0/R$ (R_0 is the dc reflectivity). In fact, the dc reflectivity varies little with lattice temperature. As is shown in Fig. 1, in the range of our measurements at $\lambda=632.8$ nm (HeNe) the variation of R_0 is less than 6%. At 294 K, $R_0=37\%$, while at 623 K the dc reflectivity becomes, $R_0=38.8\%$.[16,17] This theoretical result was verified experimentally. The reflectivity measurements (using only the probe HeNe beam) were performed throughout the temperature range from 294 to 623 K, and the signal was essentially constant. Taking into account these results, the changes of the background reflectivity R_0 have been ignored in the rest of this work. In addition, the linearity of the PMTR signal versus the laser pump intensity has also been verified.

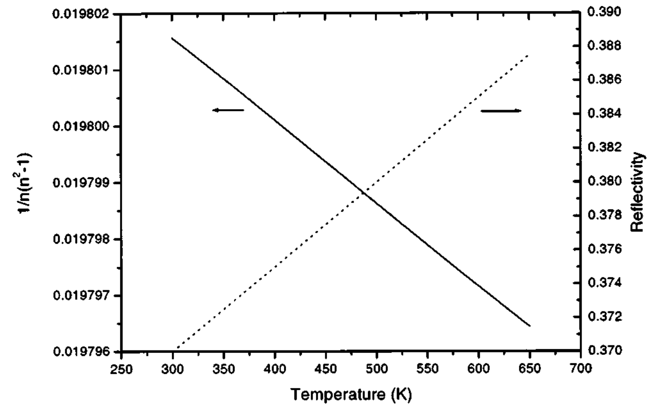

FIG. 1. $[n(n^2-1)]^{-1}$ and R_0 (for crystalline silicon) vs temperature in the range of 300 to 650 K (see Ref. 16).

III. EXPERIMENTAL PART

A. Silicon implanted and annealed samples

This article presents experimental data obtained from PMTR measurements at elevated temperatures on phosphorus implanted silicon. Silicon wafers, lightly doped with boron ($\rho\approx 20$ to 25 Ω cm), were implanted with phosphorus at 5×10^{15} $\mathrm{P}^+/\mathrm{cm}^2$ at implantation energy of 150 keV. The phosphorus ion implantation process was performed through a thin oxide layer at room temperature. Some samples were then annealed for 1 h at various temperatures, T_a, between 300 and 1100 °C in a N_2 atmosphere. After annealing, the oxide over layer was etched away and the samples were used for the experiments.

B. Photothermal experimental setup

The experimental configuration is illustrated in Fig. 2; it is similar to the one employed in the past,[4–12] with the important addition of the temperature sensing-controlling equipment. The sample is placed in the high-temperature chamber. The sample holder is isolated by a ceramic element in order to limit the heat diffusion to the surrounding area. The chamber was equipped with suitable inlet and exhaust nitrogen gas. A gas flow through the chamber during the high-temperature photothermal measurements avoided any

Downloaded 30 May 2010 to 194.42.23.188. Redistribution subject to AIP license or copyright; see http://jap.aip.org/jap/copyright.jsp

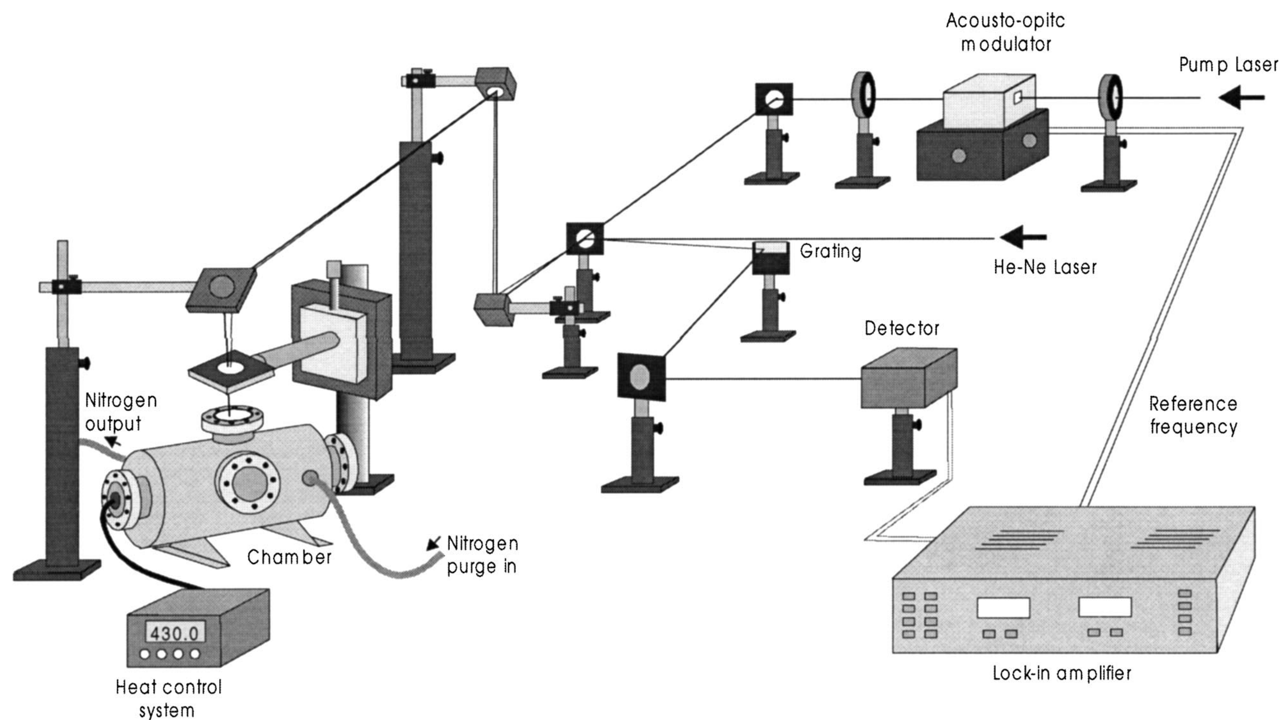

FIG. 2. Experimental setup for the laser-induced elevated temperature-dependent PMTR measurements.

oxidation of the semiconducting surface. Optical access is also available through a quartz window. The periodic sample heating was obtained with Ar^+ laser beam (488 nm), modulated by an acousto-optic device. This beam with incident power of approximately 100 mW was focused normally onto sample surface to a spot size of about 40 μm. The changes in the reflectivity of the HeNe laser beam (632.8 nm) were measured by a silicon photodiode. PMTR measurements were taken in the temperature range between 294 and 623 K and at modulation frequencies between 100 Hz and 100 kHz using an EG&G 5310 lock-in amplifier. After the stabilization of the temperature, the amplitude and phase signal were stored in a computer.

IV. EXPERIMENTAL RESULTS

Figure 3(a) shows the variation of the PMTR signal amplitude versus modulation frequency for the implanted and nonannealed silicon sample, at various temperatures in the range from 294 to 624 K. Figure 3(b) shows the variation of the PMTR phase for the same sample. As was expected in respect to the frequency, we can point out the decrease of the PMTR signal with increasing modulation frequency. The dependence of the PMTR signal on frequency is obvious and is in agreement with several simulation and experimental results presented in the past.[4–13] At room temperature (294 K), we note that the phase varies from 0° to $-35°$ in the frequency range between 100 Hz and 100 kHz. On the other hand, at 623 K, the phase varies from 0° to $-53°$. This phase shift is in agreement with several theoretical simulations performed in literature.[18,19] On the other hand, one can see that, at elevated temperatures, the phase shift increase becomes more significant. This phenomenon is more pronounced at higher frequencies. It is also evident from the slopes of Figs. 3 and 4 that the plasma wave contribution is also present even at low modulation frequencies.

Figure 4(a) shows the variation of the PMTR signal amplitude versus modulation frequency for the implanted and highly annealed (1000 °C) silicon sample, at various temperatures in the same range as before. Figure 4(b) shows the variation of the PMTR phase for the same sample. As was expected in respect to the frequency, we can point out the decrease of the PMTR signal with increasing modulation frequency.

In Fig. 5(a), we present the PMTR experimental data versus temperature at the various modulation frequencies, 1, 10, 50, and 100 kHz for the implanted and not annealed sample. We note the decrease of the PMTR signal with increasing frequency. In addition, Fig. 5(b) presents the PMTR phase versus frequency for the same temperature range. In Fig. 5(b), one can note that the PMTR phase *lag* increases as a function of temperature, especially in the case of high modulation frequencies. In fact, this phase *lag* increases, due to the fact that at higher temperatures thermal free carriers tend to occupy defect sites, thus decreasing the recombination probability of laser-generated free carriers. As a result, the free carriers have a longer lifetime thus contributing more to the PMTR signal (which explains the increase of the signal amplitude with temperature) and, therefore, they can diffusive deeper in the material, thus moving the carrier density wave centroid deeper resulting in a phase lag increase. The analysis that has been presented here is valid only in the 1D case. The aim of this work is to qualitatively explain the variation of the PMTR signal versus temperature. One can find similar results in Figs. 6(a) and 6(b) for the highly implanted sample annealed at 1000 °C.

Downloaded 30 May 2010 to 194.42.23.188. Redistribution subject to AIP license or copyright; see http://jap.aip.org/jap/copyright.jsp

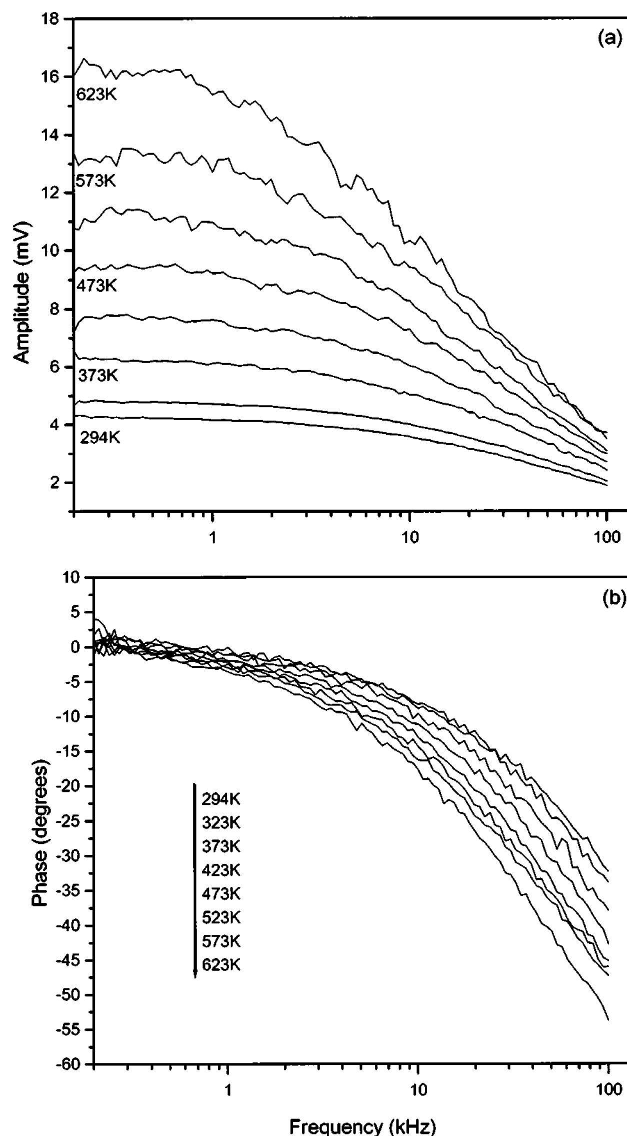

FIG. 3. PMTR signal vs modulation frequency for the phosphorus implanted and nonannealed silicon sample at various temperatures in the range of 294 to 623 K: (a) PMTR amplitude signal and (b) PMTR phase signal. (Implantation dose: 5×10^{15} P^+/cm^2; implantation energy: 150 keV.)

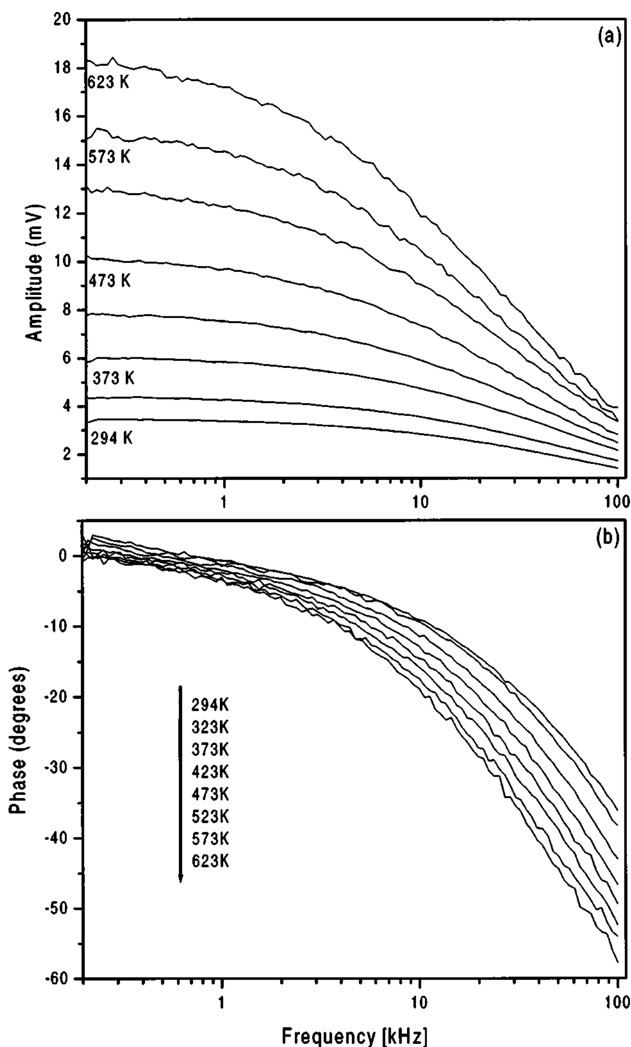

FIG. 4. PMTR signal vs modulation frequency for the phosphorus implanted and annealed silicon sample at various temperatures in the range of 294 to 623 K: (a) PMTR amplitude signal and (b) PMTR phase signal. (Implantation dose: 5×10^{15} P^+/cm^2; implantation energy: 150 keV; annealed temperature 1000 °C.)

V. DISCUSSION

A. Influence of annealing

In this section, the variation of the photothermal signal versus temperature is discussed. The discussion will be mainly limited to the Figs. 5 and 6 since these summarize the experimental results versus temperature for various modulation frequencies. As is well known in the experimental frequency range of this work, the PMTR signal is induced from a thermal as well as from a plasma component. The variation of the PMTR signal as a function of frequency was well discussed in the past but this variation at a higher temperature has not been measured. It is evident that the strong variation of electrical, thermal, and optical coefficients versus temperature makes this study of a great importance. The difference between the photothermal measurements obtained from the nonannealed and annealed samples has also been discussed in the past, the variation, however, of the PMTR signal versus experimental temperature merits discussion and analysis. The variation of the PMTR signal versus temperature is due to two main reasons: (1) The variation of the thermal conductivity and (2) the variation of the optical absorption coefficient. In order to better understand this discussion, we present Fig. 7.[20] Figure 7 shows the variation of the thermal conductivity and of the absorption coefficient in the appropriate experimental temperature range. We note that κ varies from 1.4 to 0.6 W/cm K, and α varies from 1×10^4 to 2.5×10^4 cm^{-1}, thereby increasing the amount of light energy absorbed at the surface and, consequently, the PMTR signal. Thus, one can explain the experimental results for low modulation frequencies such as 1 and 10 kHz. In fact in this case, the signal is also highly influenced by the thermal effect and thus the signal amplitude increases since the absorbed light by the sample increases drastically. For higher modulation frequencies, the signal influence of the plasma contribution becomes more important and ΔN has to be taken into account.

Downloaded 30 May 2010 to 194.42.23.188. Redistribution subject to AIP license or copyright; see http://jap.aip.org/jap/copyright.jsp

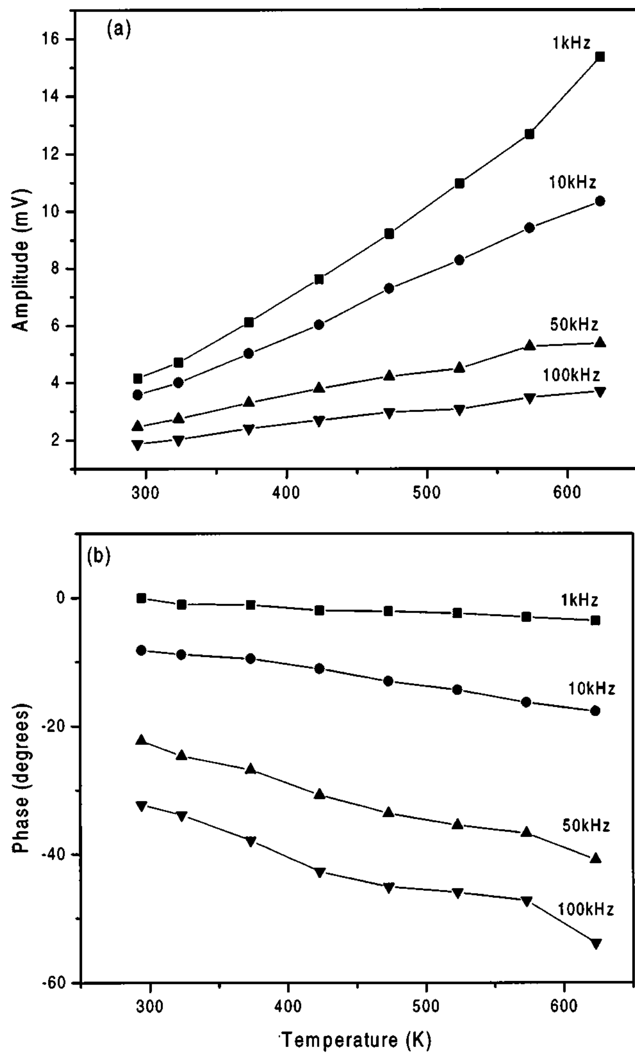

FIG. 5. PMTR signal vs temperature for the phosphorus implanted and nonannealed silicon sample at four different modulation frequencies, 1, 10, 50, and 100 kHz: (a) PMTR amplitude and (b) PMTR phase signal. (Implantation dose: 5×10^{15} P^{+}/cm^{2}; implantation energy: 150 keV.)

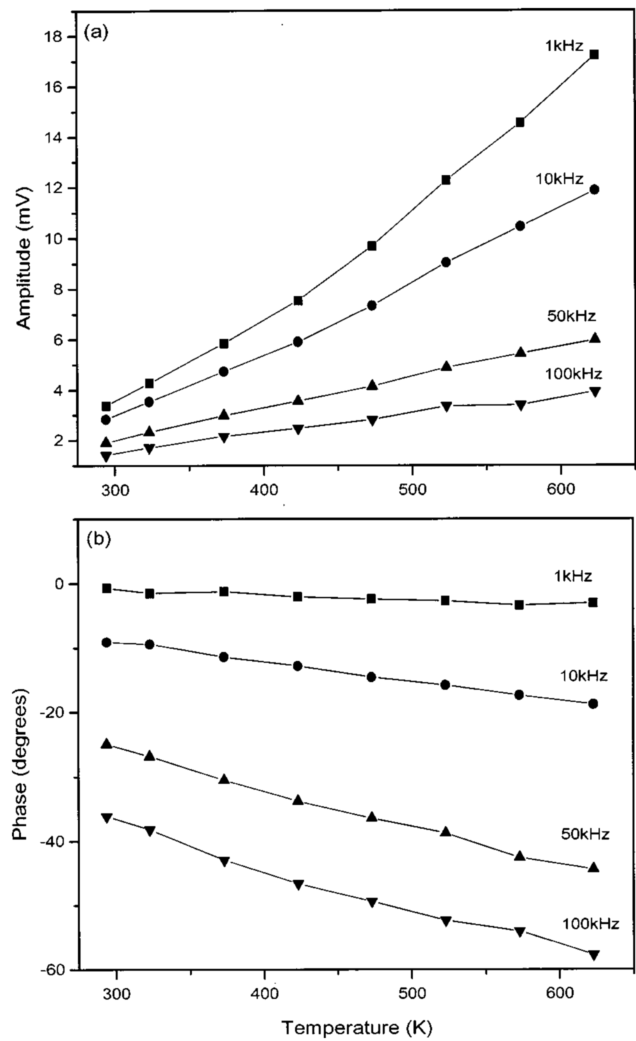

FIG. 6. PMTR signal vs temperature for the phosphorus implanted and annealed silicon sample at four different modulation frequencies, 1, 10, 50, and 100 kHz: (a) PMTR amplitude and (b) PMTR phase signal. (Implantation dose: 5×10^{15} P^{+}/cm^{2}; implantation energy: 150 keV; annealed temperature 1000 °C.)

Figure 8 shows the photothermal signal as a function of the annealing temperature, T_a, over the range of 300 to 1000 °C. These measurements are taken at room temperature for various modulation frequencies. Note that annealing at 500 °C causes a noticeable decrease of the PMTR signal, implying a significant decrease in short- and long-range disorder. In fact as is well known, for annealing at 400 °C and over, it is possible to annihilate many kinds of defects such as point defects, interstitial vacancies, impurities vacancies, and divacancies. A negative annealing is also noticeable in Fig. 8 around 700 °C. Such phenomena have also been presented in the past using PMTR in the case of arsenic implanted wafers. In this case, the negative annealing took place earlier, at around 500 °C. This may be due to the fact that in the case of arsenic, less energy is required for the formation of complex defects since arsenic is a heavier ion than phosphorus and the destroyed regions possess more defects in the neighborhood, which are required for the formation of the complex. Higher annealing temperatures

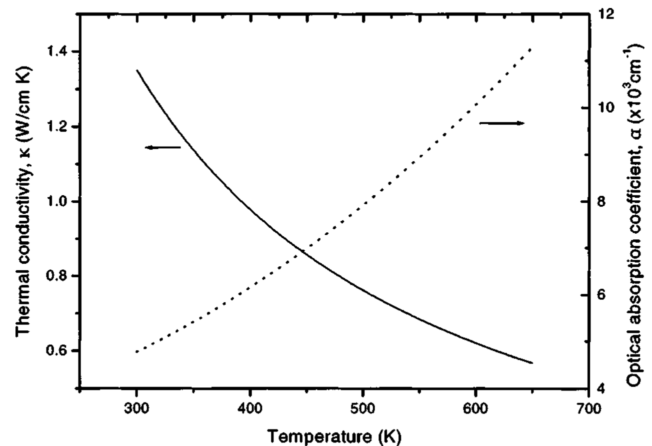

FIG. 7. Thermal conductivity and optical absorption coefficient as a function of temperature for crystalline silicon (see Ref. 20).

Downloaded 30 May 2010 to 194.42.23.188. Redistribution subject to AIP license or copyright; see http://jap.aip.org/jap/copyright.jsp

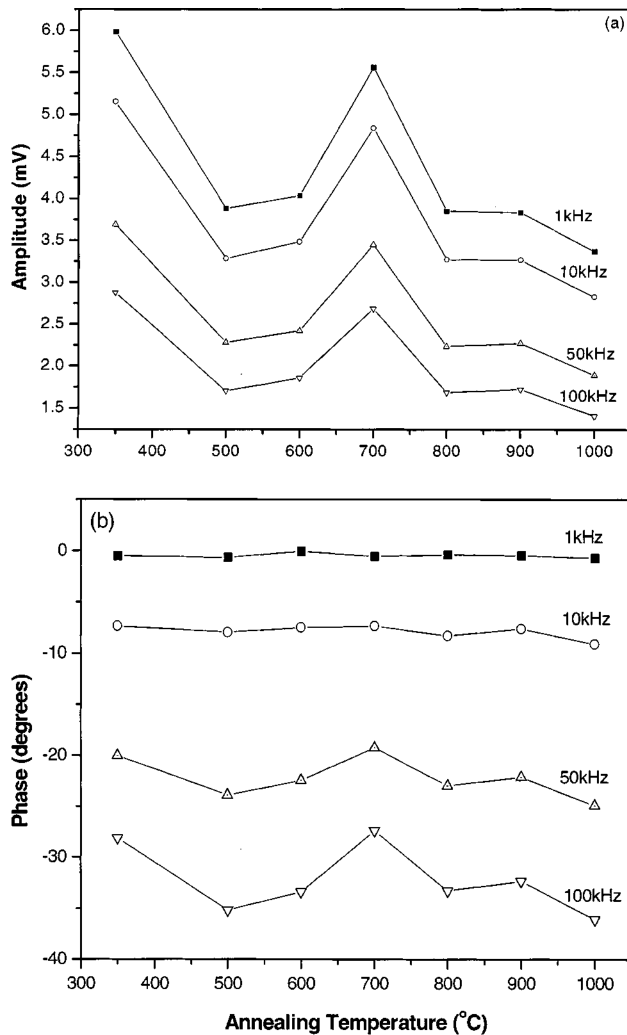

FIG. 8. PMTR signal vs annealing temperature for the phosphorus implanted silicon sample at four different modulation frequencies, 1, 10, 50, and 100 kHz: (a) PMTR amplitude and (b) PMTR phase signal. (Implantation dose: 5×10^{15} P^+/cm^2; implantation energy: 150 keV.)

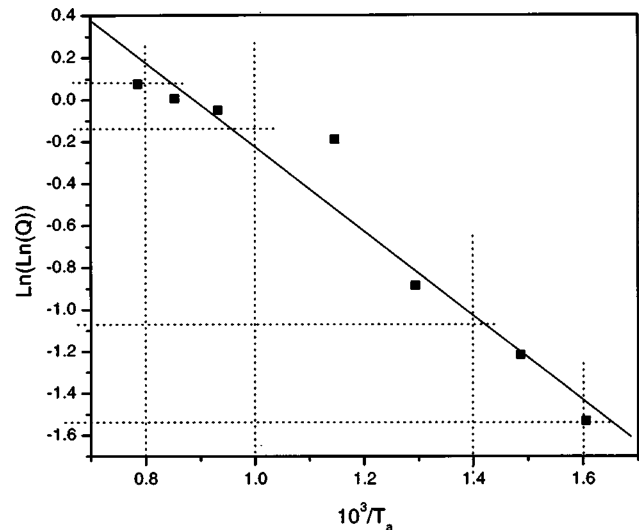

FIG. 9. Determination of the activation energy of the local annealing process by using PMTR experimental results (data taken from Fig. 8). The region corresponding to the negative annealing regime is not taken into account.

($<700\,°C$) lead to the dissociation of complex defects and the annihilation of dislocation defects.

B. Annealing kinetics of defects

In 1990, Christofides *et al.*[11] showed that the kinetics of annihilation of the damage layer, as monitored by the PMTR, are consistent with a local annealing process in which the PMTR signal could be described by the relaxation-type relationship

$$\Delta R(T_a)=(\Delta R_i-\Delta R_\infty)\exp\left(-\frac{t}{\tau}\right)+\Delta R_\infty, \tag{5}$$

where $\Delta R(T_a)$ is the PMTR amplitude signal from the annealed wafer at a given temperature, ΔR_i is the signal for the as-implanted nonannealed sample, ΔR_∞ is the signal corresponding to no implanted wafer (i.e., equivalent to a very high annealing temperature), t is the annealing duration, and τ is the relaxation time of the local annealing process. It is important to note that $1/\tau$ is the velocity constant of the annealing reaction in which the implanted ions (and/or displaced silicon atoms) migrate from interstitial to substitutional sites. $1/\tau$ can be written with an Arrhenius-type formulation, such as

$$\frac{1}{\tau}=C\exp\left(-\frac{E_a}{k_BT_a}\right) \tag{6}$$

where C is constant and E_a is the activation energy of the local annealing process. From Eqs. (5) and (6), one can easily show that

$$Q=\frac{\Delta R_i-\Delta R_\infty}{\Delta R(T_a)-\Delta R_\infty}=\exp\left[\frac{t}{C}\exp\left(-\frac{E_a}{k_BT_a}\right)\right]. \tag{7}$$

By taking the double logarithm of Eq. (7), one can obtain

$$\ln[\ln(Q)]=\Lambda-\frac{E_a}{k_BT_a}, \tag{8}$$

where Λ is constant and equal to $\ln(t/C)$.[2,21] Thus, plotting the double logarithm of Q as a function of $1/T_a$ should yield a straight line of slope $-E_a/k_B$. To construct this plot, one must ignore the part of the annealing range where the negative annealing takes place. In fact in this range, we have the formation of complex defects and the above analysis cannot cover this phenomenon. Figure 9 presents $\ln[\ln(Q)]$ versus the inverse of the annealing temperature. The measurement of the slope yields $E_a\approx0.17$ eV. According to Boltaks,[22] this activation energy corresponds to a local migration of interstitial vacancies. Hadjersi also found similar results.[23]

VI. CONCLUSIONS

The use of the PMTR technique at elevated temperatures for the characterization of semiconducting materials can be a useful technique in semiconductor technology. The main results of our study can be summarized as follows.

(1) There exists a strong influence of lattice temperature. This dependence has been explained in terms of the

Downloaded 30 May 2010 to 194.42.23.188. Redistribution subject to AIP license or copyright; see http://jap.aip.org/jap/copyright.jsp

variation of the thermal and plasma wave contributions as a function of experimental temperature.

(2) The PMTR technique has been found to be very sensitive to residual defects in a large temperature range (300 to 650 K).

(3) The activation energy of the local annealing recovery mechanism in phosphorous-damaged silicon was found to be close to 0.17 eV and corresponds to a local migration of interstitial vacancies. The same value has been calculated for various temperatures, the activation energy remains constant for the temperature range of this work.

ACKNOWLEDGMENT

The support of the Research Promotion Foundation of the Government of Cyprus under the "ΠΕΝΕΚ 14/2000" is gratefully acknowledged.

[1] H. Ryssel and I. Ruge, *Ion Implantation* (Wiley, New York, 1986).
[2] C. Christofides and G. Ghibaudo, *Semiconductors and Semimetals* (Academic, New York, 1997), Vol. 46.
[3] G. Ghibaudo and C. Christofides, *Semiconductors and Semimetals* (Academic, New York, 1997), Vol. 45.
[4] A. Rosencwaig, in *Photothermal and Thermal Wave Phenomena in Semiconductors*, edited by A. Mandelis (North–Holland, New York, 1987), Chap. 5.
[5] A. Rosencwaig, J. Opsal, W. L. Smith, and D. L. Willenborg, Appl. Phys. Lett. **46**, 1013 (1985).
[6] J. Opsal, M. W. Taylor, W. L. Smith, and A. Rosencwaig, J. Appl. Phys. **61**, 240 (1986).
[7] A. Rosencwaig, Science **218**, 223 (1982).
[8] J. Opsal and A. Rosencwaig, Appl. Phys. Lett. **47**, 498 (1985).
[9] A. Rosencwaig, J. Opsal, W. L. Smith, and D. L. Willenborg, Appl. Phys. Lett. **46**, 1013 (1985).
[10] D. Guidotti and H. M. van Driel, Appl. Phys. Lett. **47**, 1336 (1985).
[11] C. Christofides, I. A. Vitkin, and A. Mandelis, J. Appl. Phys. **67**, 2815 (1990).
[12] I. A. Vitkin, C. Christofides, and A. Mandelis, J. Appl. Phys. **67**, 2822 (1990).
[13] M. Nestoros, B. C. Forget, C. Christofides, and A. Seas, Phys. Rev. B **51**, 14115 (1995).
[14] A. Mandelis, M. Nestoros, and C. Christofides, Opt. Eng. **36**, 459 (1997).
[15] C. Christofides, A. Othonos, and E. Loizidou, J. Appl. Phys. **92**, 1280 (2002).
[16] T. Tomita, T. Kinosada, T. Yamashita, M. Shiota, and T. Sakurai, Jpn. J. Appl. Phys., Part 2 **25**, L925 (1986).
[17] S. M. Sze, *Physics of Semiconductor Devices* (Wiley-Interscience, London, 1969), Chap. 2.
[18] C. Christofides, M. Nestoros, and A. Othonos, *in Progress in Photothermal and Photoacoustic Science and Technology-Semiconductors and Electronic Materials*, edited by A. Mandelis and P. Hess (SPIE, Bellingham, WA, 2000), pp. 110–142.
[19] A. Salnick, A. Mandelis, A. Othonos, and C. Christofides, *Review of Progress in Quantitative Non-destructive Evaluation*, edited by D. O. Thompson and D. E. Chimenti (Plenum, New York, 1997), Vol. 16, pp. 371–378.
[20] J. R. Meyer, M. R. Kruer, and F. J. Bartoli, J. Appl. Phys. **51**, 5513 (1980).
[21] C. Christofides, Semicond. Sci. Technol. **7**, 1283 (1992).
[22] B. Boltaks, *Diffusion in Semiconductors* (Mir, Moscow, 1977), Chaps. 2 and 3.
[23] T. Hadjersi, Appl. Phys. Sci. **185**, 140 (2001).

Downloaded 30 May 2010 to 194.42.23.188. Redistribution subject to AIP license or copyright; see http://jap.aip.org/jap/copyright.jsp